EPS-0467
Submitted to Pa 14 and Pl 4, 11

Photoproduction of $D^{*\pm}$ Mesons in Electron-Proton Collisions at HERA

H1 Collaboration

Abstract

New results are reported on the inclusive production of $D^{*\pm}$ mesons, measured by the H1 collaboration at the ep collider HERA. The dominant production mechanism is photon gluon fusion $\gamma g \to c\bar{c}$, hence the cross section measurement can be used to constrain the gluon momentum distribution in the proton. The reconstruction of D^{*+} mesons (and its charge conjugate states) makes use of the tight kinematical constraint of the decay $D^{*+} \to D^0\pi^+$, due to the small mass difference between the D^{*+} and D^0 mesons which are detected by their decay $D^0 \to K^-\pi^+$. A preliminary ep cross section has been measured as $\sigma(ep \to c\bar{c}X) = (153 \pm 27 \pm 21 \pm 46)\, nb$ in the range $Q^2 < 0.01\,\mathrm{GeV}^2$, $159 < W_{\gamma p} < 242\,\mathrm{GeV}$. Here Q^2 is the four-momentum of the exchanged photon and $W_{\gamma p}$ the photon proton centre-of-mass energy. It is converted into a preliminary photoproduction cross section by unfolding the photon flux, yielding $\sigma(\gamma p \to c\bar{c}X) = (10.8 \pm 1.9 \pm 1.5 \pm 3.2)\,\mu b$ at an average $W_{\gamma p} = 200\,\mathrm{GeV}$. This result compares well with the predictions of next-to-leading order QCD calculations and extrapolates well from the low-energy fixed-target experiments if a rather steep increase of the gluon density at low x is assumed. First evidence for diffractive photoproduction of D^{*+} mesons is reported.

1 Introduction

The study of heavy quark production in lepton proton scattering provides an important testing ground for the standard model [1]. At the electron-proton collider HERA, heavy quarks are produced in leading order QCD by the *photon gluon fusion* process (fig. 1a),

$$\gamma g \to c\bar{c}X, \tag{1}$$

where a photon emitted by the electron and a gluon from the proton generate a $c\bar{c}$ pair. The dominant contribution is due to the exchange of an almost real photon *(photoproduction, $Q^2 \approx 0$)*. The scattered electron is either lost in the beampipe or detected at small angles. Measurements at HERA can be considered as a continuation of fixed-target *photoproduction* experiments [2], but at about one order of magnitude higher centre-of-mass energies, $W_{\gamma p} \sim \mathcal{O}(100)\,\mathrm{GeV}$. The fraction of $c\bar{c}$ events where the scattered electron is seen in the main detector *(deep inelastic scattering, $Q^2 > 4\,\mathrm{GeV}^2$)* [3], is expected to be smaller than in *photoproduction*. Other production mechanisms, as for example the production of charm in the fragmentation process, which is suppressed by the heavy mass of the charm quark, or the production by a significant intrinsic charm content of the nucleon [5], are supposed to be small.

In the *Weizsäcker-Williams Approximation* (WWA) [4], the electroproduction cross section is expressed as a convolution of the flux of photons emitted by the electron with the photoproduction cross section

$$\sigma(ep \to c\bar{c}X) = \int dy f_{\gamma/e}(y)\sigma(\gamma p \to c\bar{c}X), \tag{2}$$

where $y = E_\gamma/E_e$ represents the fraction of the energy of the photon E_γ with respect to the energy E_e of the incident lepton in the proton rest frame. The photoproduction cross section, in turn, is assumed in leading order to factorize into the photon gluon fusion parton cross section and the gluon density in the proton

$$\sigma(\gamma p \to c\bar{c}X) = \int dx_g G(x_g, \mu^2)\sigma(\gamma g \to c\bar{c}X). \tag{3}$$

Here x_g denotes the momentum fraction of the proton carried by the gluon and μ the factorization scale. Eqn. 3 can be used to extract the gluon density in leading order QCD. Recently, calculations of next-to-leading order (NLO) corrections became available [6, 7]. These were found to be substantial, but are reduced by the experimental selection cuts, which limit the acceptance to the central region only [7].

In addition, charm photoproduction can also proceed via the hadronic component of the photon *(resolved photon processes)*, where a parton inside the photon scatters off a parton inside the proton, e.g. (fig. 1b)

$$gg \to c\bar{c}X. \tag{4}$$

This process, which is known to dominate light quark production (order 90%), is expected to produce less than 10% of the charm quark pairs [7].

Estimates of the cross section strongly depend on the behaviour of the gluon density distribution of the proton at small Bjorken-x (already in leading order). Additional uncertainties arise from the renormalization and factorization scales, from the heavy quark mass, and the parton density function of the photon [8]. Heavy quark production therefore offers the possibility to probe the gluon distribution either, indirectly, by measurement of the total photoproduction cross section or distributions of pseudorapidity or transverse momentum of charmed hadrons, or directly, by the explicit reconstruction of x_g. A study based on the first method, is described here. A similar measurement has also been reported recently by the ZEUS Collaboration [9].

In the present analysis, $D^{*+}(2010)$ mesons have been reconstructed to tag heavy quark production[1]. The method makes use of the tight kinematical constraint of the decay

$$D^{*+} \to D^0 \pi_s^+. \tag{5}$$

Due to the small mass difference between the D^{*+} and the D^0 mesons, the momentum of the soft pion (π_s) in the D^{*+} rest frame is 39.6 MeV only. A better resolution is thus expected in the distribution of the *mass difference*

$$\Delta M = M(D^0 \pi_s^+) - M(D^0) \tag{6}$$

rather than in the D^{*+} mass distribution itself, whose width is dominated by the momentum resolution of the detector. In addition, due to the fact that only a small phase space region is provided, the combinatorial background is substantially reduced. The D^0 meson was searched for in the decay channel

$$D^0 \to K^- \pi^+. \tag{7}$$

The fraction of D^{*+} mesons, originating from b-decays is neglected, due to the small b-production cross section at HERA. D^{*+} mesons from decays of higher-mass charm states (e.g. D^{**}) are not separated.

Recently, much interest focused on a subclass of photoproduction events with a large gap in pseudorapidity[2] between the proton remnant jet, which is mostly disappearing into the forward beampipe, and the final state hadrons. These *diffractive* processes are interpreted as an exchange of a colour-less object with the quantum numbers of the vacuum, usually called the pomeron. The study of charm production in such processes is supposed to provide information on the structure of the pomeron.

2 Data selection and analysis

The experiment was carried out using the H1 detector [10] at the HERA storage ring at DESY. The data were collected during the 1994 running period where 27.6 GeV positrons collided with 820 GeV protons, at a centre-of-mass energy of 300 GeV.

The H1-luminosity system consists of an electron detector and a photon detector, located 33 m and 103 m from the interaction point in the electron beam direction[3],

[1] Henceforth, charge conjugate states are always implicitly included.

[2] The pseudorapidity η is defined as $\eta = -\ln\tan(\theta/2)$.

[3] H1 is using a right-handed coordinate system with the z axis pointing into the direction of the proton beam (forward), the x axis pointing towards the centre of the storage ring, and the y axis pointing upwards. The direction of the incoming electron beam is termed backward. The polar angle θ is measured with respect to the proton direction.

respectively. The luminosity is determined from the rate of *Bethe-Heitler* $ep \to ep\gamma$ Bremsstrahlungs events. The integrated luminosity used for this analysis was $L = (2.77 \pm 0.04)\, pb^{-1}$. In addition, the electron detector is used to tag photoproduction events by detecting electrons scattered at small angles.

In case of electron tagged events, the fractional energy of the photon, y, is well approximated by $y \approx 1 - (E_{e'}/E_e)$. Here E_e and $E_{e'}$ are the energies of the incoming and scattered electrons, respectively. The four-momentum transfer carried by the photon is given by $Q^2 = 4E_eE_{e'}\cos^2(\theta/2)$. It depends on the electron energies and on the angle θ between the scattered electron and the proton beam direction.

The analysis is restricted to the kinematical region $0.28 < y < 0.65$ and $Q^2 < 10^{-2}$ GeV^2, where the acceptance of the electron tagger is above 0.3 with an average of 0.6. As a consequence, the γp centre-of-mass energy range is limited to $159\,\mathrm{GeV} < W_{\gamma p} = \sqrt{4yE_eE_p} < 242\,\mathrm{GeV}$, with a mean of $W_{\gamma p} \approx 200\,\mathrm{GeV}$.

Tagged events are required to have an electron candidate with energy $E_{e'} > 4\,\mathrm{GeV}$ and to have less than $E_\gamma < 2\,\mathrm{GeV}$ deposited in the photon detector. In addition, at least one charged track candidate has to be detected by means of a multi-wire proportional chamber trigger [11] and a drift chamber track trigger [12], ensuring activity in the central detector. This strongly suppresses electron beam induced background events.

Proton beam induced background is reduced offline by requiring the event vertex to be within $\pm 40\, cm$ from the nominal interaction point along the beam direction. A further reduction is achieved by excluding events with an energy flow only into the forward region of the detector. The present analysis is based on charged particles only. These are measured by two cylindrical jet drift chambers, mounted concentrically around the beamline inside a homogeneous magnetic field of 1.15 Tesla, yielding particle charge and momentum from the track curvature in the polar angular range of $20°$ to $160°$.

For each event all possible $M(K^-\pi^+)$ mass combinations were calculated, using charged tracks with transverse momenta $p_t > 0.5\,\mathrm{GeV}$. No particle identification was applied; each particle was assumed to be a kaon or a pion. Those combinations which lay within $\pm 80\,\mathrm{MeV}$ of the nominal D^0 mass of $1.865\,\mathrm{GeV}$ were combined with an additional charged track which had a transverse momentum greater than $0.120\,\mathrm{GeV}$ and a charge opposite to that of the kaon candidate.

Figure 2 shows the distribution of the mass difference for D^{*+}-candidates with $p_t(D^{*+}) > 2.5\,\mathrm{GeV}$ for all possible triggers. Clear evidence for D^{*+} production is found as a distinct enhancement of about 500 combinations in the signal region, defined as a $\pm 2.5\,\mathrm{MeV}$ window around the expected mass difference of $145.4\,\mathrm{MeV}$. No enhancement is observed if the wrong charge combinations

$$M(K^-\pi^-\pi_s^+) - M(K^-\pi^-) \tag{8}$$

are used instead, as shown by the dashed histogram in fig 2. Fig 3 shows the mass distribution of the hypothetical D^0 candidate for events in the ΔM signal region. A clear D^0 signal is found with a width of $O(30)$ MeV.

3 Results

The production cross section in ep collisions was calculated from the observed number of D^{*+} candidates, N_{obs}, for the experimentally accessible ranges of $p_t(D^*) > 2.5$ GeV, $|\cos(\theta(D^{*+}))| \leq 0.94$ (or equivalently pseudorapidities $|\eta(D^{*+})| \leq 1.74$), $Q^2 < 0.01\ GeV^2$, and $159 < W_{\gamma p} < 242$ GeV by applying corrections according to the formula

$$\sigma(ep \to D^{*\pm}X) = \sigma(ep \to D^{*+}X) + \sigma(ep \to D^{*-}X) = \frac{N_{obs}(y,\theta)}{L \cdot B \cdot \epsilon_{tot}}, \tag{9}$$

where L denotes the integrated luminosity, $B = B(D^{*+} \to D^0\pi^+) \cdot B(D^0 \to K^-\pi^+) = 0.0273 \pm 0.0011$ [19] the decay branching fraction of D^{*+} and D^0 mesons according to eqns. (5,7), and $\epsilon_{tot} = 0.60 \pm 0.11$ the total efficiency. A Monte Carlo simulation was used to determine the efficiency for the selection cuts and the geometrical acceptance of the detector. The trigger efficiency was determined from the data itself, using independent triggers.

The number of signal events was obtained directly by subtracting the integrated wrong-sign spectrum from the observed right-sign histogram. This procedure gave the same number of events, within statistics, as a simultanous fit to signal and background events in the right-sign distribution.

For the absolute normalization, a subsample with well-understood trigger requirements was used, based on the electron tagger and tracking elements. The mass difference distribution for this sample is shown in fig. 4. The observed number of $D^{*\pm}$-candidates was corrected for electron tagger acceptance, yielding 207 ± 30 events, where the statistical error results from the subtraction of the uncorrected number of wrong-sign events from the right-sign events. A preliminary ep production cross section of

$$\sigma(ep \to D^{*\pm}X) = (4.6 \pm 0.8 \pm 0.5)\, nb \tag{10}$$

was derived in the limited kinematical region described above, and then extrapolated to the full range of (θ, p_T) by means of Monte Carlo methods. The effect of hadronization was included by using the fragmentation fraction $B(c \to D^{*+}) = 0.260 \pm 0.021$ as measured by the OPAL collaboration [18]. This leads to a preliminary total charm ep production cross section of

$$\sigma(ep \to c\bar{c}X) = \frac{1}{2}\frac{\sigma(ep \to D^{*+}X) + \sigma(ep \to D^{*-}X)}{B(c \to D^{*+})} = (153 \pm 27 \pm 21 \pm 46)\, nb \tag{11}$$

at $\sqrt{s} = 300$ GeV, $Q^2 < 0.01$ GeV^2, and $159 < W_{\gamma p} < 242$ GeV. The errors refer to the statistical, the experimental systematic, and the uncertainty due to model dependences. The statistical error includes also the uncertainty due to the limited Monte Carlo statistics.

The systematic uncertainty from the tracking trigger efficiency amounts to 5 %, whereas the track reconstruction efficiency is believed to be described by the simulation with a systematic error of less than 5 %. The branching fraction introduces an an overall error of 4 % in eqns. (9,10) and 8 % in eqns. (11,12), respectively. The systematic uncertainty from the luminosity measurement is 1.5 %. The uncertainty in the electron tagger acceptance adds another 5 % to the systematic error. Finally, an uncertainty of 7 % is assigned to the contribution of various reflections from other decay modes to the observed signal, determined by Monte Carlo methods. Adding the various uncertainties in quadrature results in a total experimental systematic error of 11.9% for the inclusive D^* cross section and 13.8 % for the $c\bar{c}$ cross section, respectively.

Further systematic uncertainties originate from the choice of structure functions and charm quark mass in the extrapolation of the cross section. All numbers are based on simulations of direct charm production processes with a charm quark mass of 1.5 GeV and assuming the GRV-LO [13] parametrization of the proton structure function. Variations of the charm quark mass by ± 0.3 GeV change the acceptance by about 20 %. Using the MRSD0' [14] parametrization of the proton parton densities, reduces the overall acceptance by about 20 %, as estimated from variations at the generator level. Within the acceptance, the total efficiency for resolved photoproduction events is about 5 % lower than for direct photoproduction events. A variation of the relative ratio resolved to direct components even up to an unlikely value of 40 % resolved to 60 % direct would change the obtained cross section value by only 2 %. The combined systematic error from these model dependences is estimated to 30 % and is quoted separately in eqns. (11,12).

The ep-cross section is converted into a preliminary γp cross section in leading order, using eqn. (2), yielding

$$\sigma(\gamma p \rightarrow c\bar{c}X) = (10.8 \pm 1.9 \pm 1.5 \pm 3.2)\mu b \tag{12}$$

at an average γp cms-energy of 200 GeV. The result is shown in fig.5 in comparison with measurements by the ZEUS collaboration (at similar $W_{\gamma p}$), and previous fixed-target experiments at lower energies. Overlaid are predictions by a NLO QCD calculation [7] with structure function parametrizations MRSG[15] for the proton and GRV-G HO [16] for the photon. The region between the upper and the lower curve represents the range of values expected due to different renormalization scales from $m_c/2$ to $2m_c$.

A search for D^{*+} production by diffractive processes was performed in a sample of "rapidity gap" events, in which *no* final state hadronic energy flow is detected adjacent to the proton remnant direction. The selection is based on "tagging" the production of forward energy with the forward "plug" calorimeter ($E_{PLUG} < 1.$ GeV in $3.54 < \eta < 5.08$), and the production of hadrons with the forward muon detector in $5.0 < \eta < 6.6$ (see ref. [20] for details). The mass difference distribution for these events is shown in fig. 6, indicating clear evidence for charm production in diffractive processes. The number of D^* candidates is not directly comparable to the total sample due to a somewhat different event selection.

4 Conclusions

A preliminary measurement of the charm photoproduction cross section has been performed through the detection of D^{*+} mesons at an average γp cms-energy of 200 GeV, yielding $\sigma(\gamma p \rightarrow c\bar{c}X) = (10.8 \pm 1.9 \pm 1.5 \pm 3.2)\,\mu b$. This value is about one order of magnitude larger than the one measured at previous fixed-target photoproduction experiments. The $W_{\gamma p}$ dependence of the photoproduction cross section is well described by NLO QCD calculations and is in favour of a steep gluon momentum distribution in the proton, as for instance implemented in the MRSG proton density parametrization. This is in agreement with measurements of the gluon density by other methods [21], e.g. the scaling violations of the proton structure function F_2, performed in deep inelastic scattering at a much higher mass scale.

Acknowledgments

We gratefully acknowledge the efforts of the HERA machine group for high-luminosity running, the DESY computer centre, and the DESY directorate for their support. We thank Stefano Frixione for many useful discussions. The non-DESY members of the collaboration wish to thank the DESY directorate for the hospitality extended to them while working at DESY.

References

[1] A. Ali *et al.,* Proc. of the HERA Workshop, DESY, Hamburg, Vol. 1 (1988), 393
A. Ali and D. Wyler, Proc. of the Workshop "Physics at HERA", DESY, Hamburg, Vol. 2 (1991), 667 (and references therein)

[2] M.S. Atiya *et al.* (CIF Coll.), Phys.Rev.Lett. 43 (1979), 414
A.R. Clark *et al.* (BFP Coll.), Phys.Rev.Lett. 45 (1980), 682
K. Abe *et al.* (SLAC HFP Coll.), Phys.Rev. D30 (1984), 1
M. Arneodo *et al.* (EMC Coll.), Z.Phys. C35 (1987), 1
J.J. Aubert *et al.*(EMC Coll.),Nucl.Phys. B213 (1983), 31;
Phys.Lett. B167 (1986), 127
M. Adamovich *et al.* (PEC Coll.), Phys.Lett. B187 (1987), 437
J.C. Anjos *et al.* (E691 Coll.), Phys.Rev.Lett. 65 (1990), 2503
M.P. Alvarez *et al.* (NA-14/2 Coll.), Z.Phys. C60 (1993), 53
D. Aston *et al.*(WA4 Coll.),Phys.Lett. B94 (1980), 113

[3] "Charm production in deep inelastic scattering at HERA",
H1 Coll., contributed paper EPS-0469 to this conference

[4] C.F. Weizsäcker, Z.Phys. 88 (1934), 612
E.J. Williams, Phys.Rev. 45 (1934), 729

[5] S.J. Brodsky, P. Hoyer, C. Peterson, and N. Sakai, Phys.Lett. 93B (1980), 451
S.J. Brodsky, C. Peterson, and N. Sakai, Phys.Rev. D23 (1981), 2745
G.A. Schuler, Nucl.Phys. B299 (1988), 21
G. Ingelman, L. Jönsson, and M. Nyberg, DESY 92-178 (1992)

[6] R.K. Ellis and P. Nason, Nucl.Phys. B312 (1989), 551
P. Nason, S. Dawson, and R.K. Ellis, Nucl.Phys. B303 (1988), 607
J. Smith and W.L. Van Neerven, Nucl.Phys. B374 (1992), 36

[7] S. Frixione *et al.,* Phys.Lett. B348 (1995), 633; CERN-TH/95-143

[8] S. Frixione *et al.,* Nucl.Phys. B412 (1994), 225; Nucl.Phys. B431 (1995), 453

[9] M. Derrick *et al.* (ZEUS Coll.), Phys.Lett. B349 (1995), 225

[10] I. Abt *et al.* (H1 Coll.), "The H1 Detector at HERA," DESY 93-103 (1993)

[11] S. Eichenberger *et al.*, Nucl.Instr.Meth. A323 (1992), 532

[12] T. Wolff *et al.*, Nucl.Instr.Meth. A323 (1992), 537

[13] M. Glück, E. Reya, and A. Vogt, Phys. Lett. B306 (1993), 391

[14] A.D. Martin, R.G. Roberts, and W.J. Stirling, Phys.Lett. B306 (1993), 145

[15] A.D. Martin, R.G. Roberts, and W.J. Stirling, RAL-94-055 (1994)

[16] M. Glück, E. Reya, and A. Vogt, Phys.Rev. D45 (1992), 3986

[17] F. Jacquet and A. Blondel, Proc. of the study for an *ep* facility for Europe, ed. U. Amaldi, DESY 79-48 (1979)

[18] R. Akers *et al.* (OPAL Coll), CERN PPE 94/217 (1994)

[19] Particle Data Group, M.Aguilar-Benitez *et al.*, Phys. Rev. D50 (1994), 1171

[20] T. Ahmed *et al.*(H1 Coll.), Phys.Lett. B348 (1995), 681

[21] I. Abt *et al.*(H1 Coll.), Phys.Lett. B321 (1994), 161
S. Aid *et al.*(H1 Coll.), DESY 95-081 (1995), DESY 95-086 (1995)

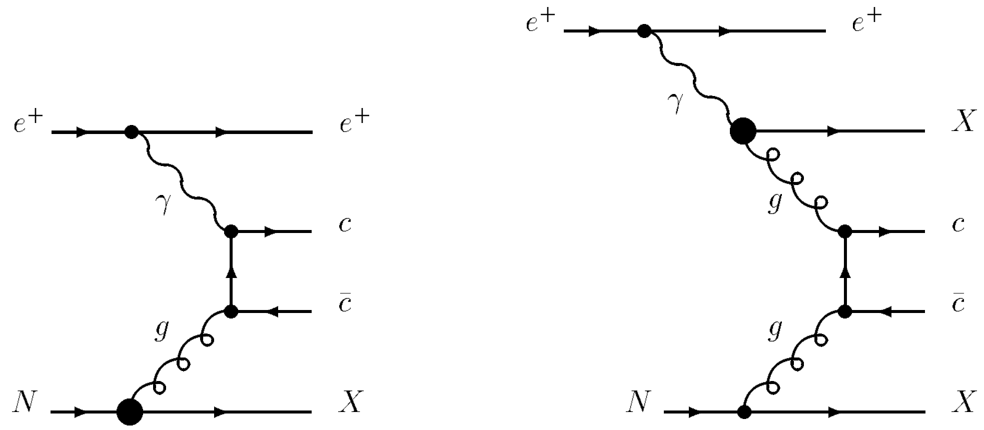

(a) direct electroproduction

(b) resolved electroproduction

Figure 1: Feynman diagrams for the electroproduction of heavy quarks through (a) direct and (b) resolved photon contributions.

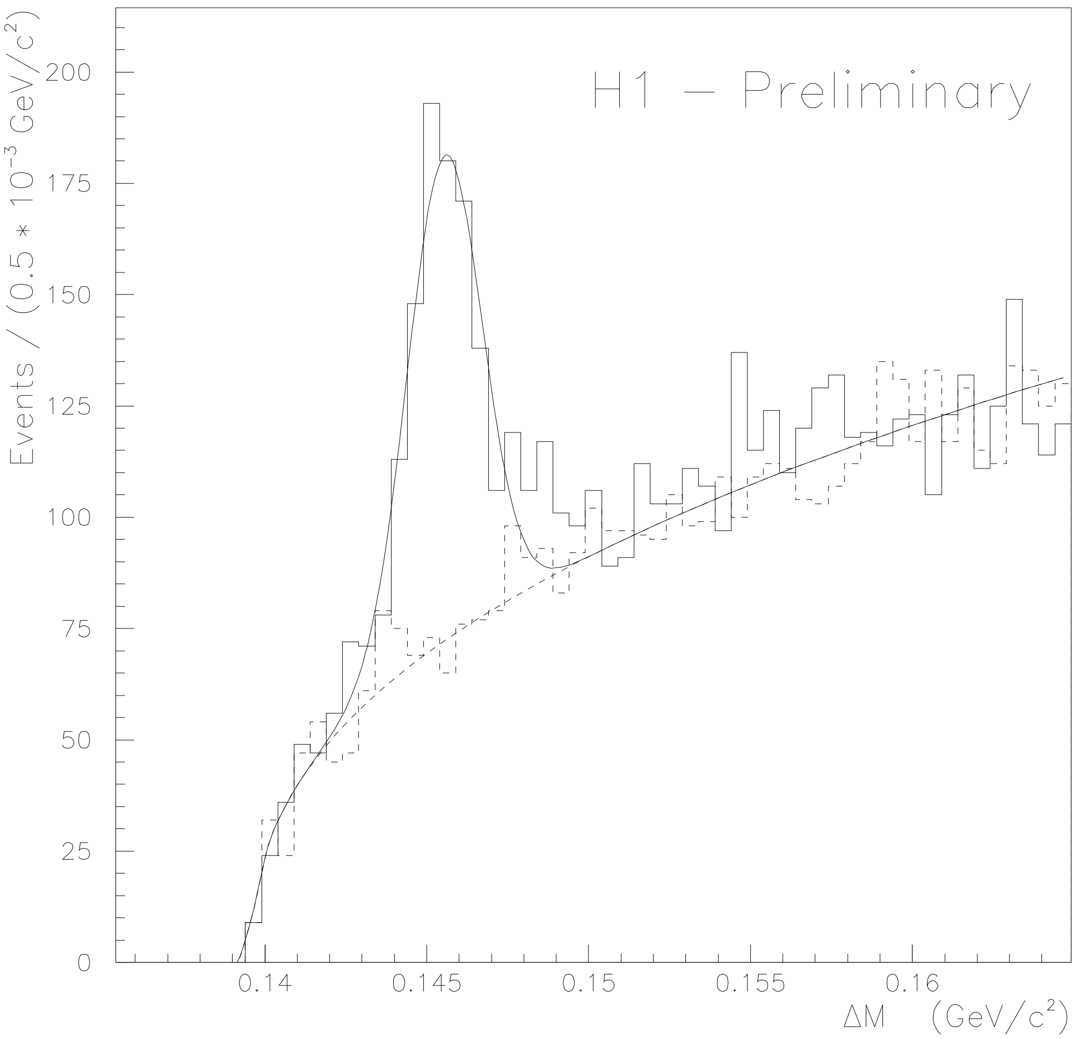

Figure 2: Distribution of the mass difference $\Delta M = M(K^-\pi^+\pi_s^+) - M(K^-\pi^+)$ for photoproduction events. The solid histogram represents the data, the dashed histogram indicates the background as obtained from wrong charge combinations. The solid line is a fit to a Gaussian for the signal plus a background term of the form $A(\Delta M - M(\pi^+))^B$.

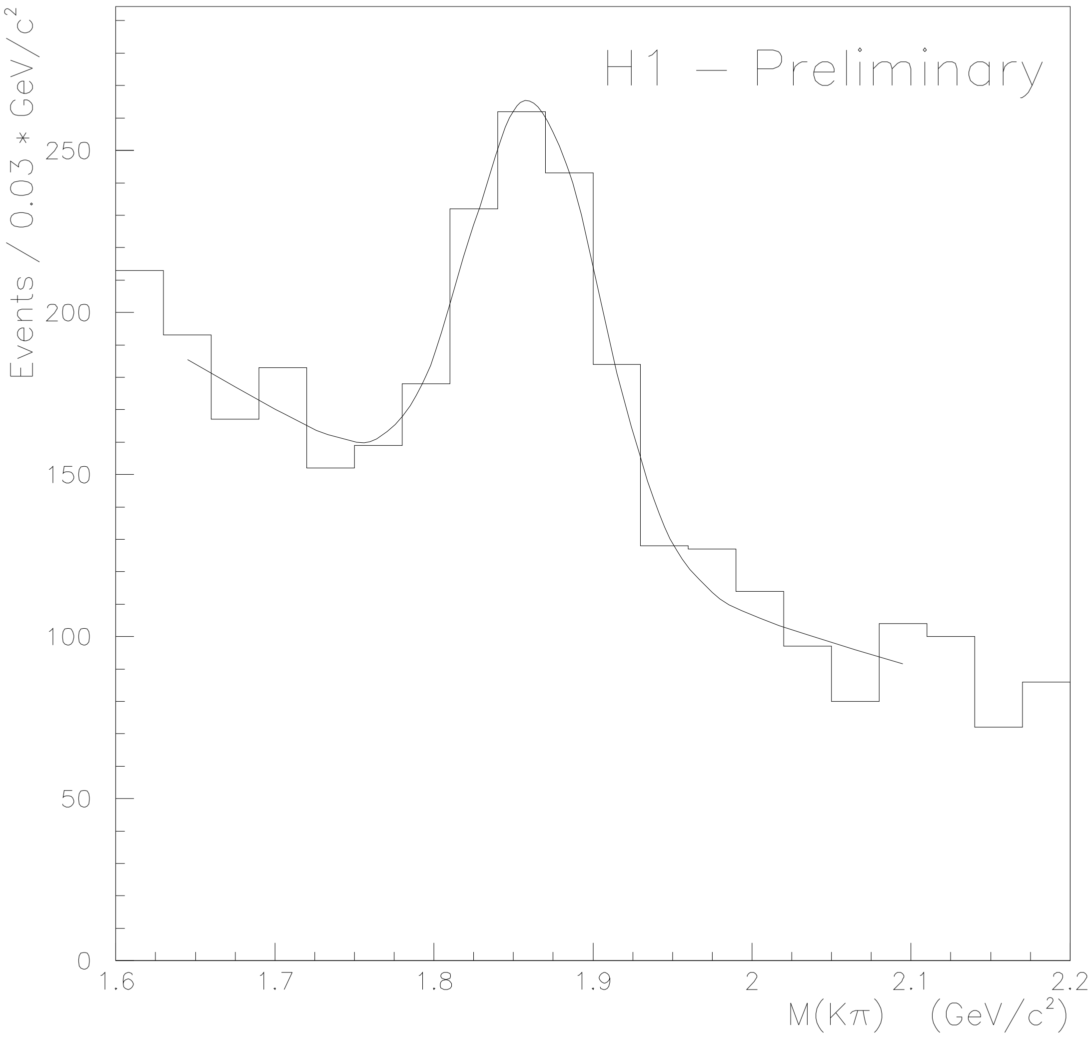

Figure 3: $K^{-}\pi^{+}$ mass distribution for candidates in the D^{*+} signal region, $143.5\,MeV < \Delta M < 147.5\,MeV$. The solid line represents the result of a fit to a Gaussian for the signal plus an exponential background term.

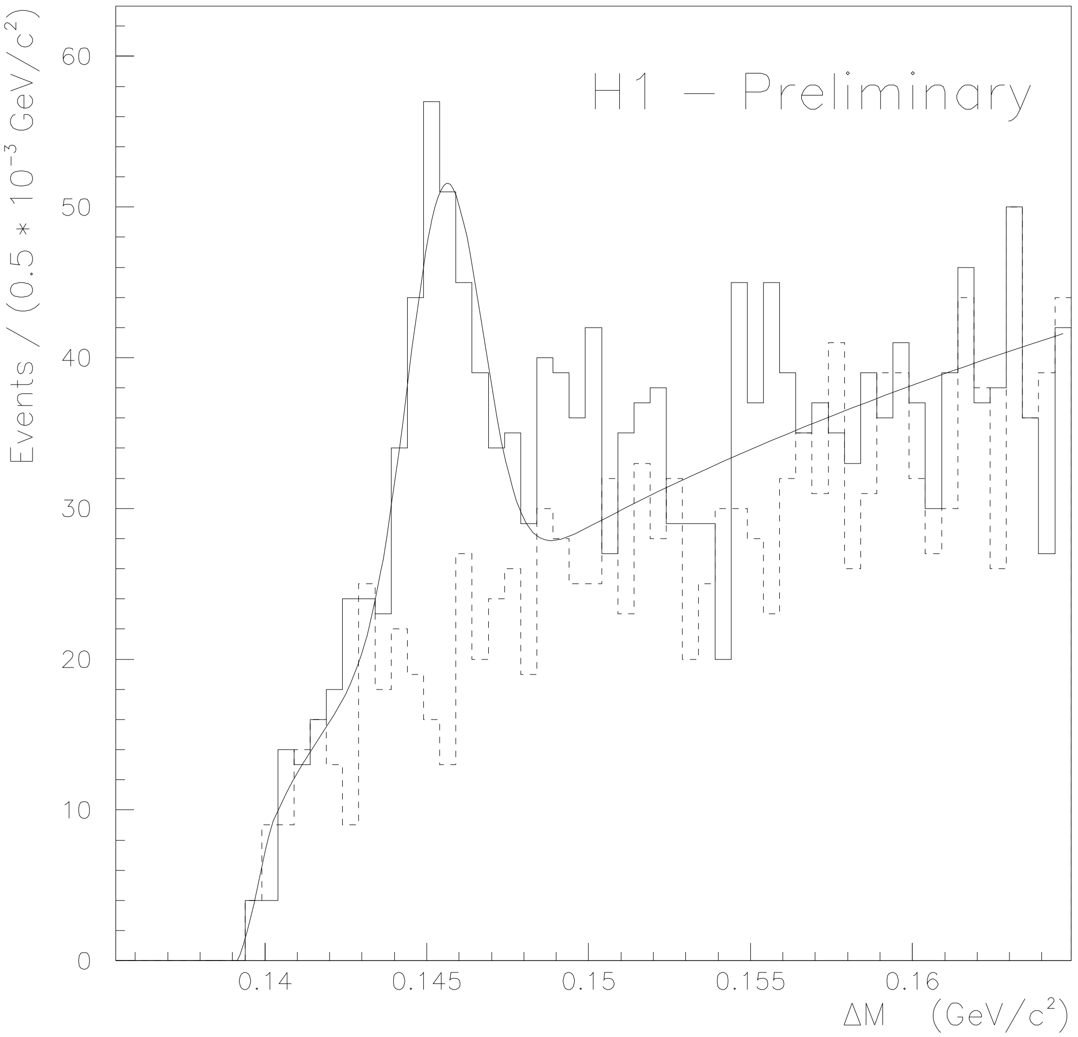

Figure 4: Distribution of the mass difference $\Delta M = M(K^-\pi^+\pi_s^+) - M(K^-\pi^+)$ for events where the scattered electron was detected at small angles. The solid histogram represents the data, the dashed histogram indicates the background as obtained from wrong charge combinations. The solid line is a fit to a Gaussian for the signal plus a background term of the form $A(\Delta M - M(\pi^+))^B$ with B fixed and A as a free parameter.

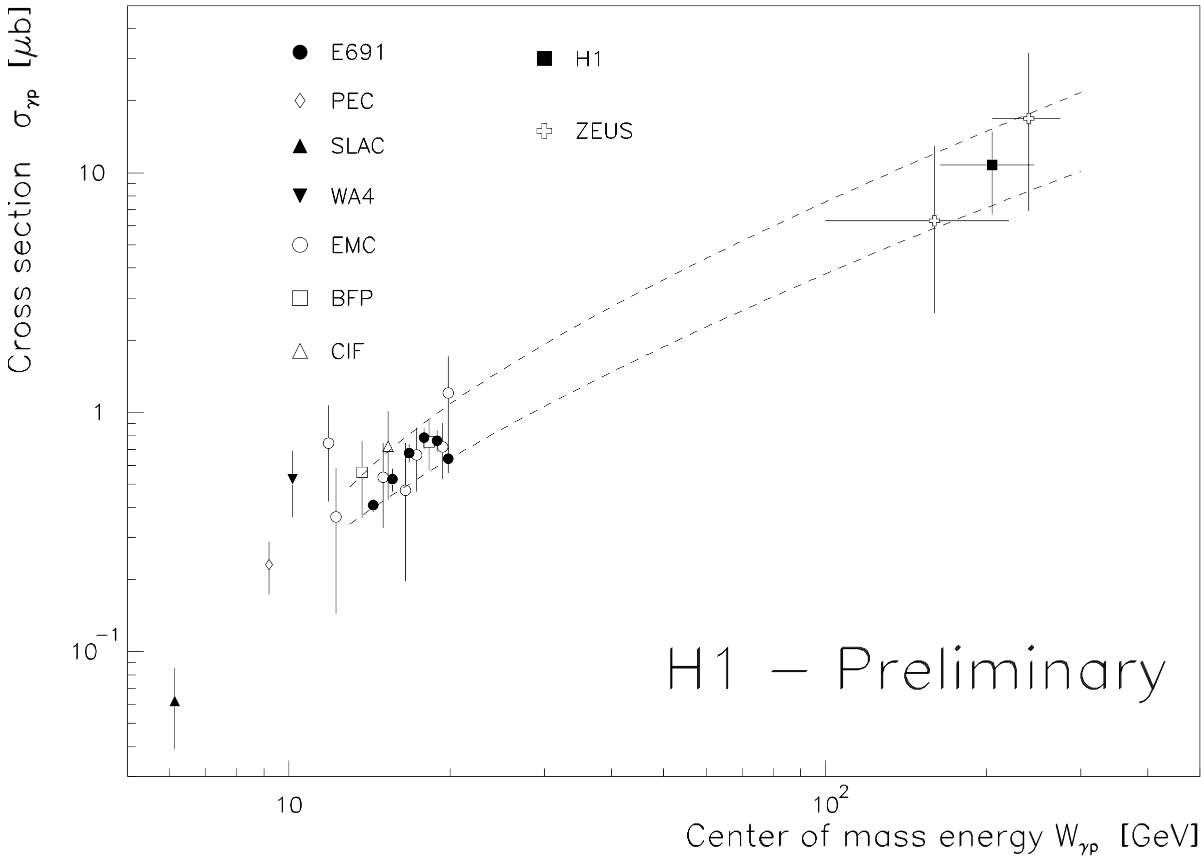

Figure 5: Total charm photoproduction cross section as a function of $W_{\gamma p}$. The solid squares represent the present analysis with the errors quoted in eqn. (12) added in quadrature, the crosses the results of the ZEUS collaboration, other symbols represent earlier measurements by fixed-target experiments. The dashed lines represent the prediction of a NLO QCD calculation using the MRSG and GRV-G HO parametrizations of the proton and photon parton densities, respectively. The upper (lower) line indicates the effect of a variation of the renormalization scale in the range $0.5 < \mu/m_c < 2.0$

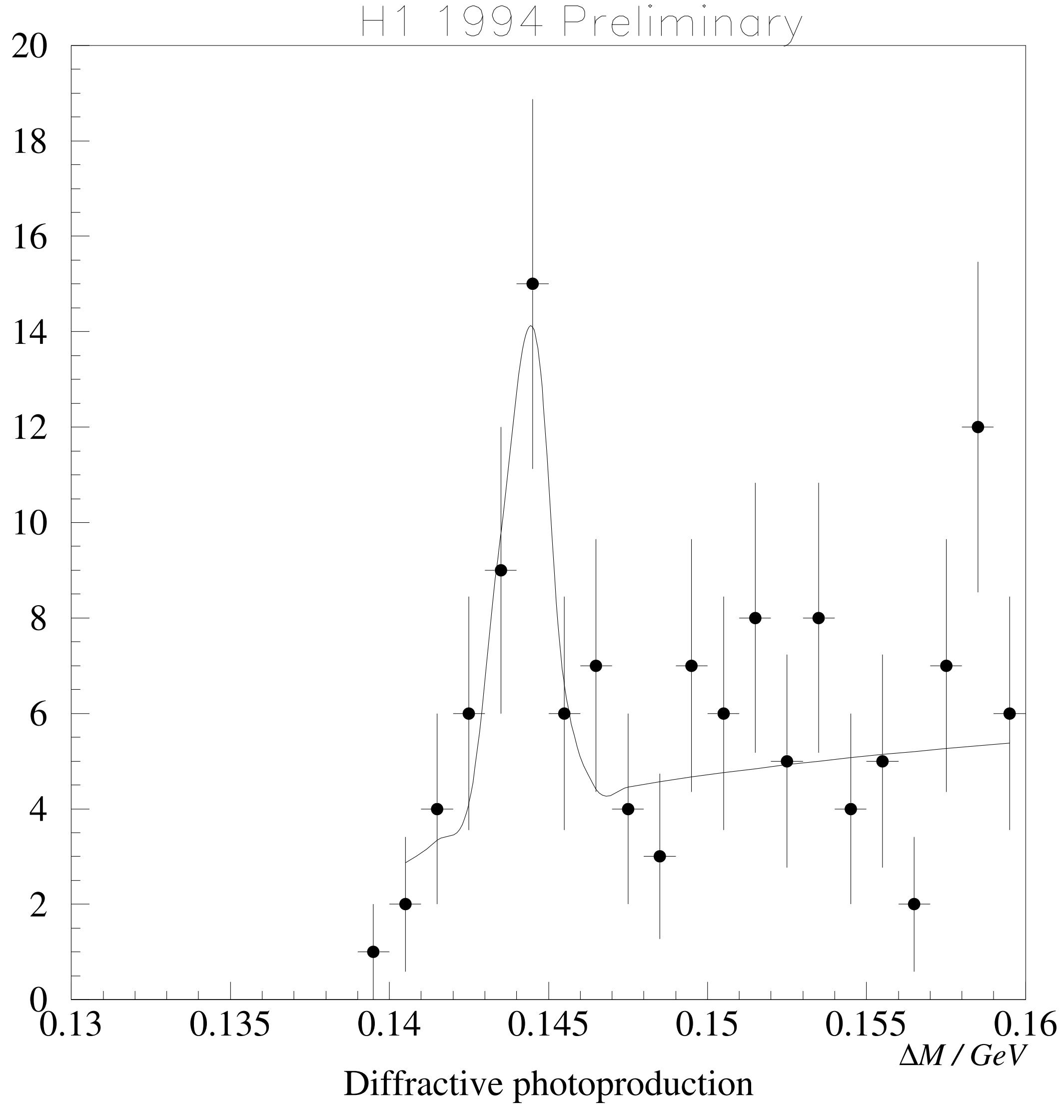

Figure 6: Distribution of the mass difference $\Delta M = M(K^-\pi^+\pi_s^+) - M(K^-\pi^+)$ for events with a rapidity gap where the scattered electron was detected at small angles. The points represent the data. The solid line is a fit to a Gaussian for the signal plus a background term of the form $A(\Delta M - M(\pi^+))^B$.